Applied Thermal Engineering 91 (2015) 408–416

Contents lists available at ScienceDirect

Applied Thermal Engineering

journal homepage: www.elsevier.com/locate/apthermeng

Research paper

Dynamic behaviors of coking process during pyrolysis of China aviation kerosene RP-3

Zhaohui Liu, Hui Pan, Song Feng, Qincheng Bi*

State Key Laboratory of Multiphase Flow in Power Engineering, Xi'an Jiaotong University, Xi'an 710049, PR China

HIGHLIGHTS

- RP-3 as an endothermic fuel was studied at temperatures up to 640 °C.
- Coking process was a combined result of a deposition process and a removal process.
- Coking process was an unsteady and dynamic one with randomness.
- Random coke buildup and removal may occur in a short time.
- Surface deposition enhanced the heat transfer at the test conditions.

ARTICLE INFO

Article history:
Received 6 July 2015
Accepted 6 August 2015
Available online 24 August 2015

Keywords:
Dynamic
Coking
Pyrolysis
Endothermic hydrocarbon fuel
Heat transfer
pressure drop

ABSTRACT

China aviation kerosene RP-3 was used as an endothermic fuel to pyrolyze in an electrically heated horizontal channel with an internal diameter of 4.0 mm at temperatures up to 640 °C, pressure of 3.0 MPa. Dynamic behaviors of coking process due to fuel pyrolysis were experimentally investigated. Coking process was considered to the net result of two simultaneous sub-processes: a deposition process and a removal process. Results indicated that coking process was an unsteady and dynamic one with randomness. During duration period of coking run, the pressure drop across the test channel and the fuel outlet temperature in some degree oscillated. The wall temperature and the pressure drop variation in a wide range became unpredictable, due to the random coke buildup and removal in a short time. However, repeated experiments were carried out to get reliable results of some regular patterns of coking process. The pressure drop exponentially increased and the wall temperature rapidly changed at the initial stage of coking run; and the pressure drop linearly increased but the wall temperature nearly achieved steady state at the following stages. Opposite to the general realization that coke is a thermal resistance layer to reduce heat transfer, surface deposition enhanced the heat transfer during pyrolysis of RP-3 at the test conditions.

1. Introduction

China aviation kerosene RP-3, as a model substance of endothermic fuel, was being intensively investigated in the recent years, especially since 2009, due to the application of endothermic fuel as a coolant in the regeneratively cooling minichannels of scramjet. The studies involved its thermophysical properties [1–8], heat transfer characteristics [9–14], surface coke deposition [15–20], effects of deposits on heat transfer [15,21,22], and other related issues [23–25].

Xu et al. [1] and Deng et al. [2,3] experimentally measured RP-3's thermal conductivities at temperatures of $285 \leq T/K \leq 513$ and pressures of $0.1 \leq P/MPa \leq 5$ [1], viscosities at $298 \leq T/K \leq 788$ and $2.33 \leq P/MPa \leq 5$ [2], densities at $295 \leq T/K \leq 796$ and $0.1 \leq P/MPa \leq 5$ [3], and specific heat capacities at $292 \leq T/K \leq 824$ and $2.4 \leq P/MPa \leq 6$ [4]. Wang et al. [5,6] determined RP-3's critical properties by the critical opalescence phenomenon observed in flow visualization. Aviation kerosene is a very complex fuel mixture, consisting of hundreds of hydrocarbon compounds. Due to the difficulties to measure the properties at high temperatures and the lack of experimental data, many surrogate fuel models [7,10,26,27] were proposed to predict fuel properties. Xu et al. [8] analyzed and compared different models involving single component n-decane, three-component [7], four-component [26], six-component [27], and

* Corresponding author. Tel./fax: +86 (0)29 82665287.
E-mail address: qcbi@mail.xjtu.edu.cn (Q. Bi).

http://dx.doi.org/10.1016/j.applthermaleng.2015.08.033
1359-4311/

Nomenclature

D	diameter, mm
L	length, mm
U	voltage, V
I	electrical current, A
M	mass flow rate, g/s
T	temperature, °C
$T_{f,inl}$	inlet fuel temperature, °C
$T_{f,out}$	outlet fuel temperature, °C
T_w	wall temperature, °C
t_{coke}	duration period of coking run, min
P	pressure, MPa
ΔP	pressure drop across the test channel, kPa
ΔP_b	pressure drop at the beginning of duration period of coking run, kPa
ΔP_e	pressure drop at the ending of duration period of coking run, kPa
q	heat flux, kW/m^2
q_{eff}	effective heat flux imposed to fuel flowing through the test channel, kW/m^2
η	thermal efficiency

ten-component [10] with experimental data [2–4]. Results indicated that the surrogate model with four components [26] was the best choice for thermophysical property calculations under the test conditions, with fluid temperatures up to 650 K at various supercritical pressures. Though the pseudo-critical temperature can be well predicted, the calculated properties using the four-component surrogate model [26] still had considerable errors within 10–40% except the density prediction with errors of less than 10%. The considerable disagreement can probably be attributed to two reasons [9]. One is that the components of China RP-3 aviation kerosene differ from shipment to shipment; the other is that chemical reactions may occur at high temperature due to the thermal oxidation and cracking, which is not considered in the current models.

Convective heat transfer characteristics of RP-3 were numerically simulated [9,10] and experimentally investigated [10–14]. Influences of radial property variation, buoyancy, and acceleration on heat transfer deterioration (HTD) were investigated under conditions relevant to an active cooling system for scramjet applications [9]. Buoyancy and acceleration effects on HTD increase as mass flow rate decreases. Buoyancy and radial property variation produced HTD for upward flow at mass flow rate $G = 500$ kg/s m^2, in which case the maximum temperature difference between wall temperature and fuel temperature reached 480 K at heat flux $q = 500$ kW/m^2. While $G = 1600$ kg/s m^2 and the ratio of heat flux to mass flow rate $q/G > 410$ J/kg at 4.5 MPa, onset of HTD occurred due to radial property variation, but the buoyancy effect can be ignored. Zhong et al. [10] found that convective heat transfer was greatly enhanced when the fuel temperature near wall exceeded 600 K. Zhang et al. [11,12] and Deng et al. [13] investigated the normal, enhanced, and deteriorated heat transfer in a 1.8 mm internal diameter channel. Li et al. [14] found that heat transfer can be augmented when the wall temperature rose over the pseudo-critical temperature along the flow direction, but at the initial heating section the opposite result was obtained. The Nusselt number at supercritical pressure was only related to the Reynolds number after the heat transfer was enhanced.

Though fuel pyrolysis can provide numerous endothermic heat sink for the actively or regeneratively cooling of hypersonic vehicles, the coke fouling produced meanwhile is a serious problem difficult to be solved. Fouling has been described as the major unresolved problem in heat transfer [28], which can seriously deteriorate heat transfer capacity. The coke deposition from chemical reaction fouling is an extremely complex phenomenon, which may be fundamentally characterized as a combined, unsteady state, momentum, heat and mass transfer problem with chemical, solubility, and corrosion processes.

Surface coking characteristics of RP-3 were investigated [15–22]. Coke deposition under stable and vibration conditions were studied at 127–450 °C and 5 MPa in a 1.8 mm internal diameter channel for 35 h deposition duration period [15]. The vibration with practical frequency of 566–600 Hz in the combustion chamber can significantly inhibit the exponential growth of flow resistance by reducing coke formation compared to the stable condition. The pyrolytic deposition rate of RP-3 at temperatures up to 700 °C increased along the tube length, but gradually decreased with extension of duration time in 20 min [16]. Conversion rate and heat sink of catalytic cracking of RP-3 were evidently heightened compared with the thermal cracking [17]. A numerical simulation for pressure effects on thermal cracking of RP-3 under supercritical conditions was conducted by the modified Kumar–Kunzru chemical kinetics model consisting of one primary reaction and twenty-three secondary reactions [18]. The conversion rate of RP-3 was proportional to the pressure when the thermal cracking occurred adequately. At pressures ranging of 3–7 MPa, coke deposition was proved to be inhibited by the increasing pressure [19]. Effects of mass flow rate on oxidation deposition were investigated at temperatures of 127–427 °C and pressure of 5 MPa [20]. Results indicated that oxidation deposition amount increased, but the deposition rate (deposition amount per fuel mass) decreased with the increasing mass flow rate. Surface coke deposition increases the flow resistance through the flow passage, and meanwhile the coke layer has a low thermal conductivity of 0.038–0.19 W/(m K) [29], therefore decreases the heat transfer capacity. The effect of coke deposition on heat transfer can be divided into three regions according to the deposition profile along the flow direction: stable heat transfer region at the tube entrance with low fuel temperature, deteriorated heat transfer region at the middle of the tube with peak coke deposition, and short term enhanced heat transfer region at high fuel temperature [21,22]. Liu et al. [23,24] and Guo et al. [25] investigated the thermal cracking and coke deposition of RP-3 in the presence of initiator additives and coke inhibitors.

In the previous report [30], we made efforts to quantitatively describe the functional relationship between coke deposition and hydraulic resistance increase, which can be used to on-line evaluate the coking characteristic of endothermic hydrocarbon fuel. But as the previous literature [31,32] reported that coke deposition was more difficult to be quantitatively described by heat transfer behaviors. We also found that the coking surface thermal performance was completely different (all the cases can happen to increase, decrease or no significant change) after coke deposition, attributed to the coke patterns, coke thickness and the surface roughness of coke deposition [33]. During pyrolysis of endothermic fuel, the flow and thermal instability always occurred. In this study using RP-3 as an endothermic fuel, we concentrate on the dynamic behaviors of coking process during its pyrolysis. Through the dynamic analysis of flow resistance and thermal performance, the coking characteristics of RP-3 are expected to be better described than before.

2. Experimental section

2.1. Test facilities

The experimental facilities were described in detail in our previous literature [30,33–38]. Fig. 1(a) shows the test sections or the

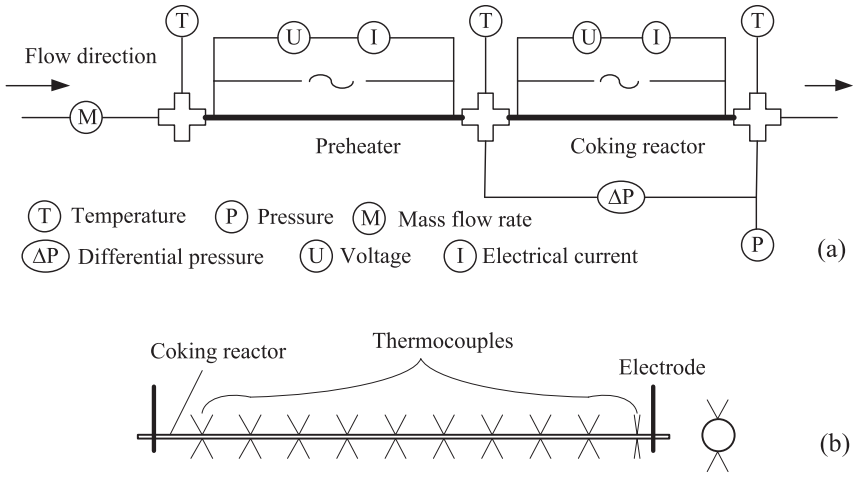

Fig. 1. Schematic diagram of (a) the test sections and (b) the coking reactor.

chemical reaction reactors including a preheater and a coking reactor, which are two electrically heated stainless steel (China SS321, Material: 1Cr18Ni9Ti) channels both with an internal diameter of 4.0 mm. The stainless steel channels were purchased from Xi'an Changtai Precise Alloy Ltd. in China. The preheater with a heated length of 900 mm was used to achieve different fuel inlet temperatures of the coking reactor, which had a heated length of 500 mm. Compared to the test channels used before [30,33] with internal diameters of 1.0 mm and 2.0 mm, the bigger diameter channel here was designed to realize longer duration period for coking run. Therefore more coke deposition formed on the inside surface of the coking reactor, which would be benefit to obtain more reliable results of its flow influence and thermal performance.

The coking reactor was resistance heated by low voltage (U < 220 V) and high alternating current (I = ~300 A) through the metal tubing. The voltage and current were measured by true RMS transmitters. The fluid inlet and outlet temperatures of the test channel were measured by type K sheathed thermocouples with external diameters of 1.0 mm, which were immerged into the flow passage. Some 20 type-K thermocouples (TC) with external diameters of 0.2 mm were spot-welded onto the outside surface of the coking reactor for measuring outside wall temperatures. In order to fully understand the heat transfer behaviors, the TCs were distributed at 10 cross sections with intervals of 50 mm along the coking channel, seen in Fig. 1(b). At each cross section two TCs were set symmetrically on the top and the bottom of the test channel. Also the two symmetrical TCs can ascertain if the temperature measurements are right, which is important for the unpredictable temperature variation during coking duration. The pressure drop across the coking reactor and the pressure at the outlet were measured by Rosemont 3051 pressure transducers. A pump before the test sections provided fuel with constant mass flow rate, which was measured by a Corioris mass flow meter before fuel entering the coking reactor. The fuel pyrolyzed and deposition accumulated in the coking reactor surface, and then the reacted fuel was cooled in a condenser. After that, a back pressure regulator was used to control the operating pressure in the experimental system. All of the measured data were collected by Isolated Measurement Pods IMP 3595 data acquisition system and input into industrial personal computer by every 0.6 s.

2.2. Measurement method for deposition and its validation

After coking run, the coke deposition amount in the coking channel was off-line measured by gravimetric method, which was always being used for coke analysis of RP-3 [15,19–22]. The coking channel was cut into sections. At each TC point location a length of 30 mm section was used for coke amount measurement. The 20 mm section remained between the adjacent TC point was cut along the axial into two halves. The ultrasonic cleaner was used to remove the coke deposition in the 30 mm coking channel sections, which were weighed twice by an electrical balance with a precision of 0.01 mg before and after the ultrasonic cleaning. The mass difference between the twice measurements was considered to be the quality of coke deposition on the inner surface.

Through the sections cut along the axial, it was found that the coke deposition of RP-3 at the test conditions was much loose and nearly dropped naturally and completely from the channel surface. The coke structure was not as compact as that obtained during pyrolysis of other endothermic fuels at higher temperature of 750 °C in our previous studies [30,33]. The coke deposition in the latter cases stuck tight on the inner reaction surface. The loose coke deposition provided the feasibility of the ultrasonic cleaning. Three coking run experiments were conducted, and the pressure drops at the ending of the coking run and the correspondence total coke amounts in the coking channel obtained by the above gravimetric method were demonstrated in Fig. 2. Coking run was conducted at a given fuel inlet, outlet temperature, pressure and mass flow rate. The pressure drop through the coking reactor changed with deposition accumulating. Therefore the pressure drop variation reflected the growth of deposit. The agreement between the pressure drop and the coke amount validated the measurements.

2.3. Data reduction and uncertainty analysis

The measured parameters included fuel inlet temperature $T_{f,inl}$, fuel outlet temperature $T_{f,out}$, outside wall temperatures T_w along the test channel, pressure drop ΔP through the test channel, pressure P at the outlet of the test channel, heating voltage U and alternating current I, and mass flow rate M. In discerning the thermal balance of heating power and heat loss to the environment, the effective heat flux q_{eff} imposed to fuel can be determined by Eq. (1).

$$q_{eff} = UI\eta/(\pi DL) \quad (1)$$

The heating efficiencyη, which was measured by the heating balance method as a function of the channel's outside surface temperature. The heating efficiency was measured as η < 10.0% at all operating conditions in this study. The considerable heat efficiency contributed to high fuel temperatures (which led to high

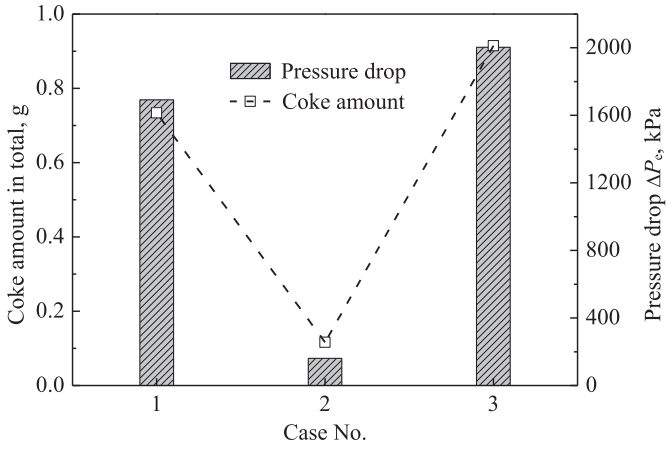

Fig. 2. Relationship between the pressure drop and the coke deposition amount.

wall temperatures up to 850 °C), a relatively low mass flow rate and a large surface area for the test channel. The heating efficiency was experimentally measured by heating the preheated channel without fuel employed. In that case, the heating power was indicated as equal to the heat loss at the corresponding constant wall temperature at a steady state. The results of the heat efficiency test were calibrated and validated by using the coking channel at fuel temperatures from 25 °C to 650 °C. The heating power imposed on the coking channel was indicated as its heat loss while the inlet and outlet fuel temperatures were kept accordant.

The standard uncertainties of the measured parameters were estimated based on standard deviation of the experimental data. All the results of experimental parameters were determined by averaging a group of experimental data in a 30-s continuous data collection. The standard uncertainties of the voltage U and current I were both 1.0%. The uncertainty of the heated length L and internal diameter D of the test channel were 0.5 mm and 2.1%. Therefore the standard uncertainty of the effective heat flux q_{eff} was estimated as 2.5% according to Eq. (1). The standard uncertainties of the measured temperatures were ±0.2 °C at a temperature of $T < 200$ °C, ±0.5 °C at 200 °C $\leq T <$ 500 °C, and ±1.0 °C at 500 °C $\leq T <$ 800 °C. The standard uncertainty of mass flow rate was 0.5%, and that of pressure drop and pressure were both 1.0%.

3. Results and discussion

Aviation kerosene is a very complex fuel mixture, consisting of hundreds of hydrocarbon compounds. Its' components include 53 wt.% alkanes, 39 wt.% cycloalkanes, 5 wt.% benzenes, and 3 wt.% naphthalenes [10]. The critical temperature and pressure are 372.4 °C and 2.4 MPa respectively, measured by Wang et al. [6]. In this study RP-3 was used as endothermic fuel to pyrolyze at temperatures up to 640 °C and at a supercritical pressure of 3.0 MPa. Dynamics including flow influence and thermal performance of surface coke deposition was experimentally investigated.

3.1. Operating conditions

Table 1 gave the detailed parameters for different coking runs. In order to get reliable results, we repeated the experiments at the nearly same operating conditions. The fuel with mass flow rate of 1.0 g/s entered the coking reactor at ambient temperature, flew through the heated reactor, then exited at fuel outlet temperature $T_{f,out}$ ranging of 600–640 °C and pressure of 3 MPa. The coking run was carried out for hours until severe coke deposition occurred in the coking reactor. The pressure drop across the test channel at the beginning ΔP_b and the ending ΔP_e of the coking run were presented. At Case No. 1, the pressure drop increased to 1614 kPa from 3.3 kPa in 35 min. At Case No. 2, the pressure increased to 256 kPa at the ending from 4.9 kPa at the beginning. However, during coking run, the pressure drop went up to 1535 kPa in 26 min, but then suddenly decreased to 3.8 kPa in 1 s, then again increased with time but more slowly than before. At Case No. 3, the pressure drop increased to 2012 kPa from 6.3 kPa in 56 min. The coking processes will be discussed in detail in the following sections.

3.2. Dynamics of pressure drop during coking processes

The overall fouling process is usually considered to be the net result of two simultaneous sub-processes: a deposition process and a removal process [28]. Fig. 3 is a schematic demonstration of the fouling processes. The coke forms in the bulk of the fluid, and deposits on the deposit–fluid interface. Removal of the deposit may occur, and then the coke returns to the bulk of the fluid again. Therefore the growth of the deposit on the surface depends on the difference between the deposition and removal rates. And the coke fouling process is a dynamic and unsteady one in which the fluid flow velocity, surface temperature, surface material, surface roughness, and fluid properties are identified as the most pronounced effects on fouling.

As Fig. 4(a) showed that the pressure drop profiles with respect of time were clearly divided into three stages. At the initial stage, 0–9 min for Case No. 2 and 0–18 min for Case No. 3, the pressure drop had low values of 5–100 kPa but exponentially increased by 16–20 times, shown in Fig. 4(b). The exponentially fitted equations are shown in Eqs. (2) and (3) for Case No. 2 and Case No. 3 respectively. And the increasing rates of pressure drop were 62.1 and 36.9 kPa/min respectively at the end of the initial stage.

At the following stage, 9–26 min for Case No. 2 and 18–56 min for Case No. 3, the pressure drop detached the low value region and linearly increased from 100 kPa to 1500 kPa and 2000 kPa. The linearly fitted equations are shown in Eqs. (4) and (5) for Case No. 2 and Case No. 3 respectively. The increasing rates are 10.5 and 12.6 kPa/min respectively. Results indicated that as the transition of the first stage and the second stage, the increasing rate of pressure drop substantially reduced. It may occur or not for the third stage that after suddenly falling into the original value in the beginning of coking run, the pressure drop again exponentially increased as the first stage, show in Fig. 4(c) for the Case No. 2. The exponentially fitted equation is shown in Eq. (6). The suddenly fall of the pressure drop meant that the surface deposition was integrally peeled off from the inside wall and flushed away from the reactor.

$$\Delta P = e^{2.53-0.128t+0.0132t^2} \tag{2}$$

$$\Delta P = e^{2.71-0.187t+0.0405t^2} \tag{3}$$

$$\Delta P = 10.5t - 7.6 \tag{4}$$

Table 1
Operating conditions for different coking runs at $P = 3.0$ MPa and $M = 1.0$ g/s.

No.	$T_{f,in}$, °C	$T_{f,out}$, °C	q_{eff}, kW/m^2	t_{coke}, min	ΔP_b, kPa	ΔP_e, kPa
1	12.5	603.8	277	35	3.3	1614
2	12.1	604.2	272	65	4.9	256
3	20.1	637.3	293	56	5.0	2012

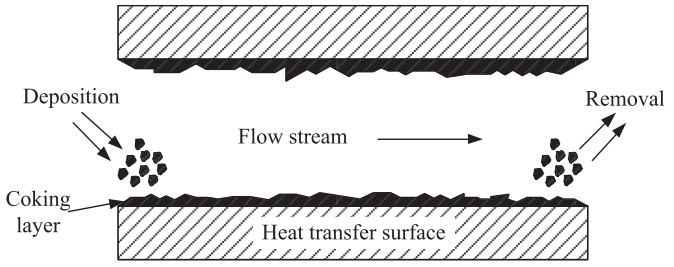

Fig. 3. Coke fouling processes.

$$\Delta P = 12.6t - 185.5 \quad (5)$$

$$\Delta P = e^{-1.59+0.144t-5.68t^2} \quad (6)$$

It indicated that the coking process in a small scale of time was an unsteady and dynamic one. The growth curves of the pressure drop were not smooth even in the initial stage, as Fig. 4(b) and (c) showed that there were some pulse waves in the curves. And Fig. 4(a) showed that the pressure drop may also suddenly increase by a considerable magnitude like that at 9 min and 24 min of the Case No. 2. The discontinuous and sudden change of the pressure drop were the result of the partial or integral removal of the deposit due to "spalling" or "sloughing" to be followed for a short time by a rapid buildup of deposit [28]. That gives an explanation why the pressure drop and pressure soared in a sudden during fuel pyrolysis in a 2 mm internal diameter minichannel in our previous study [33]. The coking process was also a random one. Though it is ascertained there were obviously three stages during the coking run, the moments for the transitions of different stages were unpredictable, and also the sudden removal and buildup of deposit were hard to be known in advance. At Case No. 1 and Case No. 3, the third stage did not happen, even though the pressure drop achieved a considerable high level much bigger than the highest value at Case No. 2. Though the growth curves of the pressure drop exponentially or linearly increased in the three stages, the growth rates of the pressure drop much varied.

3.3. Dynamics of wall temperature during coking processes

Fig. 5 showed the wall temperature at TC1 point with time during repeated coking run of Case No. 1, No. 2, and No. 3. Both the wall temperatures at the top and the bottom of the test channel were presented. The wall temperatures rose and fell synchronously at the top and bottom of the test channel for all the three locations, which confirmed the accuracy measurements of wall temperature, especially at the moments the wall temperature rapidly changed.

The wall temperatures at the top were always higher than those at the bottom with temperature differences of 25–100 °C, which was a result of the buoyancy effect of the horizontally distributed coking reactor on the heat transfer performance. The bulk fuel

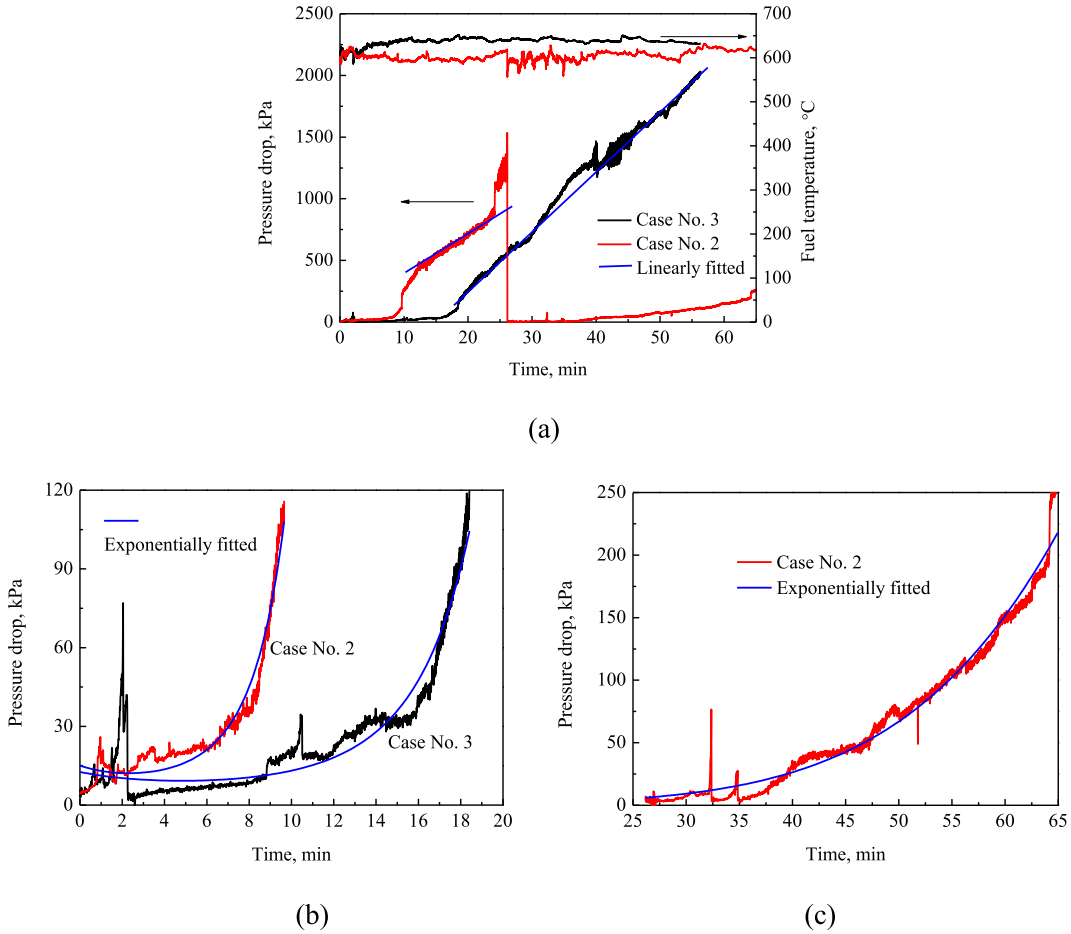

Fig. 4. Dynamics of pressure drop during coking run at Case No. 2 and No. 3. (a) Pressure drop with respect of time during the whole coking duration. (b) Pressure drop exponentially increased with time at the initial stage. (c) Pressure drop exponentially increased with time at the end stage of Case No. 2.

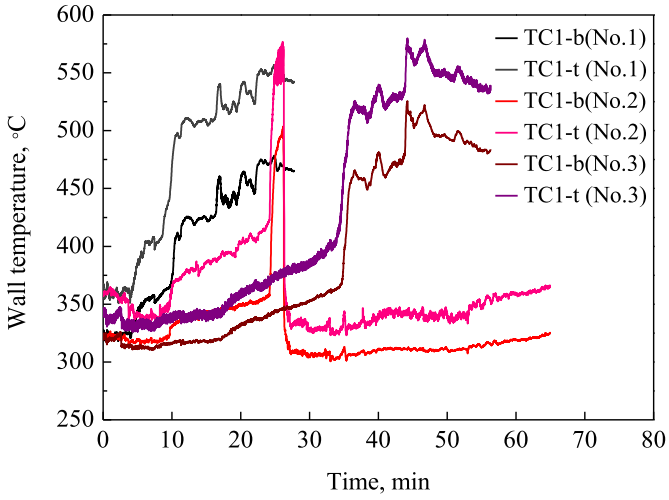

Fig. 5. Comparison of wall temperatures with time between repeated coking runs. TC1 is the wall temperature at the first thermocouple location along the flow direction; b and t mean locations at the bottom and top of the horizontal test channel.

temperature at TC1 location was around 100 °C, therefore the radial temperature variation ranged from 200 °C to 450 °C.

It indicated that the wall temperature variation with time was also randomness and unpredictable but accordant with the pressure drop variation. At the beginning, the wall temperatures were around 340 °C. But during coking run, the wall temperature would be an unpredictable value in a range of 300–600 °C. The lowest temperature of 300 °C can be at the ending of the coking run, such as in Case No. 2, due to the coke layer integrally peeled off. The highest temperature can be reached in 10 min after the start of coking run, such as in the Case No. 1. But in the Case No. 3, the highest temperature was reached after 40 min. The wall temperature may change very quickly, increased 100 °C in 1 min, or suddenly decreased by 200 °C.

Though the coking processes were unpredictable and with much randomness, it also had some regular patterns for the pressure drop and also for the wall temperature. There were also clearly three stages for the TC1 wall temperature during the coking run. In the beginning (2 min for Case No. 1, 10 min for Case No. 2, 30 min for Case No. 3), the wall temperature slowly increased. In the following stage, the wall temperature may suddenly rose to a high value like heat transfer deterioration, which happened for all the three Case (Case No. 1 at 10 min, No. 2 at 24 min, No. 3 at 35 min). In the third stage, after a sudden rose, the wall temperature achieved a slow increase plateau but with fluctuations like "saw tooth", which was a reflection of the dynamics of coke deposition and removal [28]. And it was noted the steady temperature of the plateau was close for the different cases. The steady state meant that the deposition rate nearly balanced with the removal rate. In Case No. 2, the agreement of the pulse at 24–26 min between wall temperature and pressure drop validated the measurements.

Fig. 6 showed all the wall temperature at the top of the channel with respect of time during the coking run No. 2. It was found that the wall temperature tended to achieve steady state in the first 15 min, while the wall temperature decreased drastically except at TC1 and TC2. Though the pressure drop continued to increase at the time of 10–24 min, shown in Fig. 4(a), the wall temperature hardly changed meanwhile. The temperature changing rate deceased with time. After 55 min, the wall temperatures at all the TC points tended to be steady.

At time of 24 min, the wall temperature at TC1 began to increase rapidly, then suddenly decreased at the time of 26 min to the original temperature at the beginning of coking run. Accordant to the dynamics of pressure drop at 26 min, all the temperature tended to return to the original values, seen in the data curves at 0 min and 27 min in Fig. 7. At the beginning, deposition enhanced the heat transfer, and the wall temperature decreased. After the coke layer peeled off, the wall temperature tended to be recovered. In the following process, the wall temperature repeated the processes in the beginning again to decrease with time due to the re-accumulating of deposition, but the steady state temperature was much lower than the first time, seen in Fig. 7.

3.4. Coke effects on heat transfer during coking run

Three repeated experiments, Case No. 1, No. 2, and No. 3, were carried out at the nearly same operating condition. The wall temperature profiles along the test channel at the beginning and ending of coking run are shown in Fig. 8(a). The wall temperature at the beginning showed good respectabilities, especially for Case No. 1 and No. 2. At the entrance, the wall temperatures at TC1 and TC2 were below the critical temperature. Between TC2 and TC3, deteriorated heat transfer happened, the wall temperature rose quickly by nearly 500 °C.

Comparison of the wall temperatures at the beginning with those at the end of coking run was conducted. It was found that except wall temperatures at TC1 and TC2, the wall temperatures at the other TC points decreased. The deteriorated heat transfer was eliminated in some degree. The wall temperatures along the test channel became more uniformity, for that the low wall temperature increased and the high wall temperature decreased. The wall temperature behaviors at TC1 and TC2 for Case No. 2 were a result of that the coke layer was peeled off during coking run, which was analyzed above.

The temperature differences between the wall temperature at the beginning and the ending are shown in Fig. 8(b) together with the coke amount profiles along the test channel. It seemed that the difference of the coke deposition amount has limited influence on the heat transfer performance. The heat transfer was enhanced and the temperature difference was close at all the three cases, even though the coke amount achieved 110 mg/cm^2 at the peak, which meant that there was a coke quality of 1.09 g in per cm^3 volume of the coking channel. It was accordant with that the wall temperatures were only affected by coke deposition at the first 15 min, even though the pressure drop kept linearly increased therefore the coke deposition kept accumulated at the second stage, the wall temperature hardly changed, shown in Fig. 6. Tao et al. [15] reported similar results that wall temperature kept increased with the same scales during different coking runs regardless of the coke amounts in the range of whatever 0.5–3.5 or 5–55 mg/cm^2 in 1.8 mm internal diameter channels. In our experiments the coke amounts were in the range of 0.5–5.0, 0.5–50, and 0.5–110 mg/cm^2 for the Case No. 2, No. 1 and No. 3 respectively. The opposite point was that coke deposition deteriorated the heat transfer in the former report [15]. In our study, the total thermal resistance to heat transfer is decreased during the first stages of coke fouling due to the surface roughness resulting from initial deposition. The limited influence of coke deposit on heat transfer at the following stages should be a result of its porous structure, in which the gasified fuel can flow through easily. Therefore the heat transfer was enhanced throughout the coking process.

3.5. Oscillation caused by coke deposition

During coking run, oscillations of parameters were observed. Fig. 9 showed the oscillations of fuel outlet temperature and pressure drop through the coking reactor at Case No. 2. The

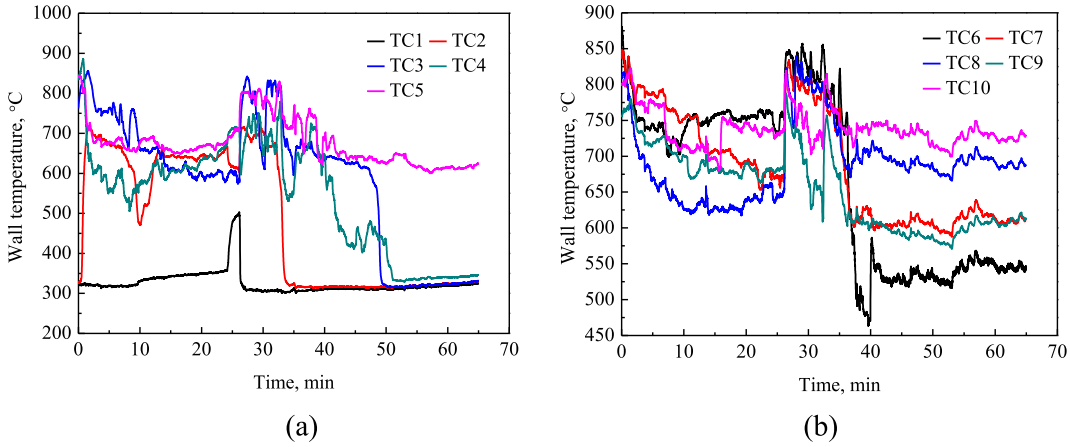

Fig. 6. Wall temperature variations with time during the coking run of Case No. 2.

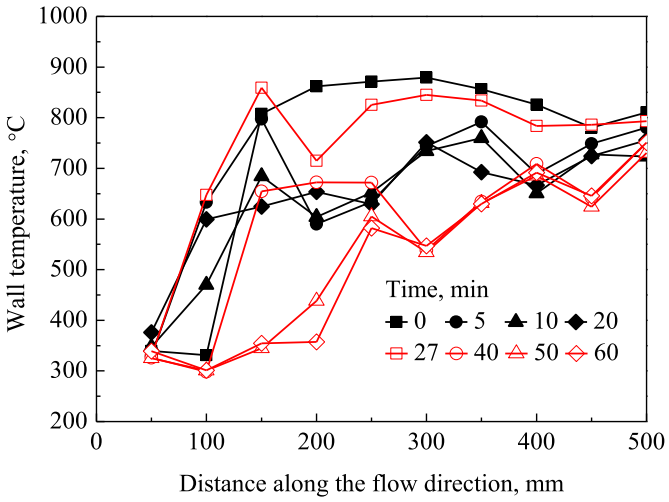

Fig. 7. Wall temperature profiles during the coking run of Case No. 2.

oscillation values of fuel outlet temperature were determined by Eq. (7), where $dT_{f,out}(i)$ represents the oscillation magnitude at the ith data collection point, $T_{f,out}(i)$ denotes the fuel outlet temperature at the ith data collection point. The oscillation values of pressure drop were determined by Eq. (8), where $d\Delta P(i)$ denotes the pressure drop oscillation magnitude at the ith data collection point.

During coking run all the experimental data were collected continuously with intervals of 0.6 s.

$$dT_{f,out}(i) = T_{f,out}(i) - T_{f,out}(i-1) \quad i = 1, \ldots n \tag{7}$$

$$d\Delta P(i) = \Delta P(i) - \Delta P(i-1) \quad i = 1, \ldots n \tag{8}$$

The fuel temperature oscillation was found to be always less than 10 °C at a fuel temperature of 600 °C. But the pressure drop oscillation can go to ±200 kPa at a pressure drop of 1600 kPa. The oscillation values for temperature were opposite to those for pressure drop. At the point the coke peeled off, the pressure drop fell to a least value from the biggest value, and then began to slowly increase again. But the fuel temperature oscillation increased to the biggest value, and then decreased with time. It indicated that as the deposition accumulated, the temperature oscillation decreased, but the pressure drop oscillation increased. The other parameters had no significant oscillation observed. The oscillations were also accordant with the three stages of the coking process. In the beginning of the first stage, fuel temperature oscillated with big magnitude, meanwhile the wall temperature dramatically decreased. At the transition of the first stage to the second stage, pressure drop oscillation significantly augmented with pressure drop increasing rate rapidly reduced. The oscillation magnitude and the increasing rate of pressure drop both maintained during the second stage.

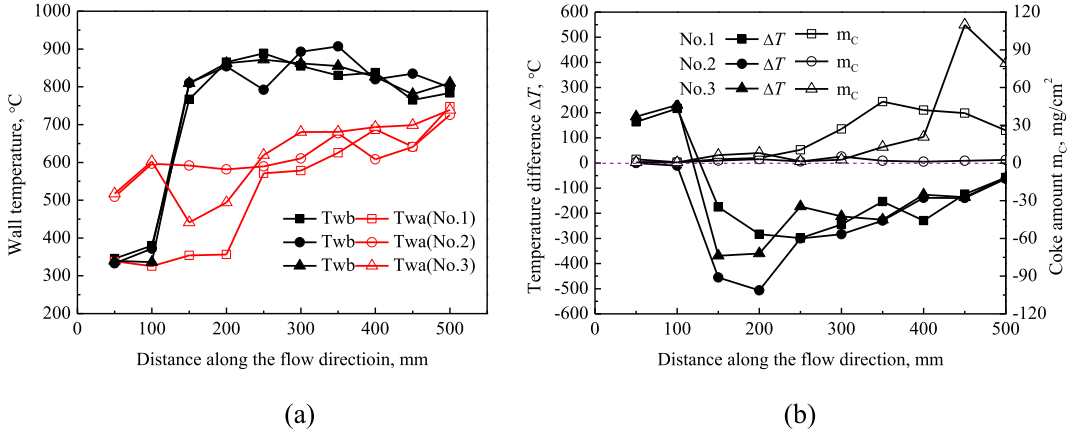

Fig. 8. Thermal effect of coke deposition during the coking run.

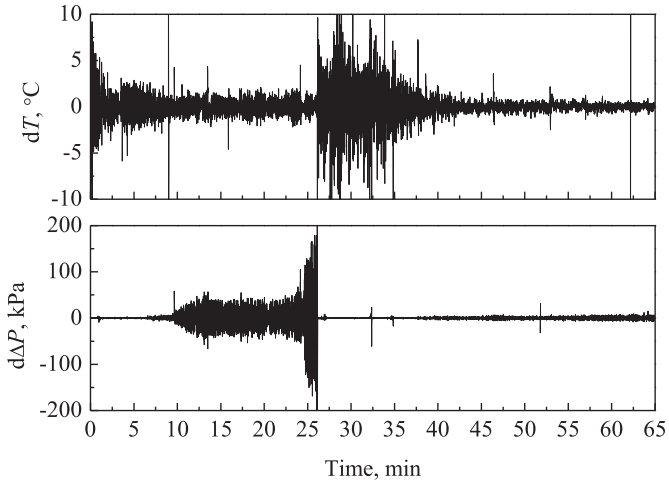

Fig. 9. Oscillations during the coking run.

4. Conclusion

China aviation kerosene RP-3 was used as an endothermic fuel to pyrolyze at temperatures up to 640 °C in an electrically heated horizontal channel with an internal diameter of 4.0 mm. Dynamics of the coke deposition during the coking run were investigated. It concluded as follows.

(1) The coking process in a small scale period was an unsteady, dynamic, and random one. During coking run, the wall temperature and pressure drop variation due to coke deposition can be in a wide range of 300 °C and 2000 kPa respectively at the test conditions, which depended on the random process of coke buildup and coke removal.
(2) The coking process had some regular patterns. The pressure drop exponentially increased and the wall temperature rapidly changed at the initial stage of coking process. Then the pressure drop linearly increased but the wall temperature nearly achieved steady state and hardly changed at the following stage. During the coking process, the pressure drop and fuel temperature oscillated. The pressure drop oscillation magnitude increased with an increase amount in coke deposition, but which was opposite for the temperature oscillation.
(3) The partial or integral coke removal, and the buildup of coke deposition in a short time made the coke process unsteady. The pressure drop and wall temperature may rise or fall in a considerable big multitude accordant to the coking process. The coke deposition enhanced heat transfer between the coke surface and the bulk fluid at the test conditions, but the coke amount in a wide variety range resulted limited influence on heat transfer performance after the initial stage of coking process.

Acknowledgements

This study was sponsored by the National Natural Science Foundation of China (Grant No. 21306147), the China Postdoctoral Science Foundation (Grant No. 2013M532044) and the Fundamental Research Funds for the Central Universities. Their financial support is gratefully acknowledged.

References

[1] G.Q. Xu, Z.X. Jia, J. Wen, H.W. Deng, Y.C. Fu, Thermal-conductivity measurements of aviation kerosene RP-3 from (285 to 513) K at sub-and supercritical pressures, Int. J. Thermophys. 36 (2015) 620–632.
[2] H.W. Deng, C.B. Zhang, G.Q. Xu, B. Zhang, Z. Tao, K. Zhu, Viscosity measurements of endothermic hydrocarbon fuel from (298 to 788) K under supercritical pressure conditions, J. Chem. Eng. Data 57 (2012) 358–365.
[3] H.W. Deng, C.B. Zhang, G.Q. Xu, Z. Tao, B. Zhang, G.Z. Liu, Density measurements of endothermic hydrocarbon fuel at sub- and supercritical conditions, J. Chem. Eng. Data 56 (2011) 2980–2986.
[4] H.W. Deng, K. Zhu, G.Q. Xu, Z. Tao, C.B. Zhang, G.Z. Liu, Isobaric specific heat capacity measurement for kerosene RP-3 in the near-critical and supercritical regions, J. Chem. Eng. Data 57 (2011) 263–268.
[5] N. Wang, J. Zhou, Y. Pan, H. Wang, Determination of critical properties of endothermic hydrocarbon fuel RP-3 based on flow visualization, Int. J. Thermophys. 35 (2014) 13–18.
[6] N. Wang, J. Zhou, Y.H. Pan, Wang, Experimental investigation on flow patterns of RP-3 kerosene under sub-critical and supercritical pressures, Acta Astronaut. 94 (2014) 834–842.
[7] X. Fan, G. Yu, Analysis of thermophysical properties of Daqing RP-3 aviation kerosene, J. Propul. Technol. 27 (2006) 187–192.
[8] K.K. Xu, H. Meng, Analyses of surrogate models for calculating thermophysical properties of aviation kerosene RP-3 at supercritical pressures, Sci. China Tech. Sci. 58 (2015) 510–518.
[9] Z.Q. Liu, J.H. Liang, Y. Pan, Numerical analysis of heat transfer deterioration of China RP-3 aviation kerosene in a circular tube at supercritical pressures, in: 11th AIAA/ASME Joint Thermophysics and Heat Transfer Conference, 16–20 June 2014. Atlanta, GA.
[10] F.Q. Zhong, X.J. Fan, G. Yu, J.G. Li, C.J. Sung, Heat transfer of aviation kerosene at supercritical conditions, J. Thermophys. Heat Transf. 23 (2009) 543–550.
[11] C.B. Zhang, G.Q. Xu, L. Gao, Experimental investigation on heat transfer of a specific fuel (RP-3) flows through downward tubes at supercritical pressure, J. Supercrit. Fluids 72 (2012) 90–99.
[12] C.B. Zhang, H.W. Deng, G.Q. Xu, W. Huang, K. Zhu, Enthalpy measurement and heat transfer investigation of RP-3 kerosene at supercritical pressure, J. Aerosp. Power 25 (2010) 331–335.
[13] H.W. Deng, K. Zhu, G.Q. Xu, Z. Tao, J.N. Sun, Heat transfer characteristics of RP-3 kerosene at supercritical pressure in a vertical circular tube, J. Enhanc. Heat Transf. 19 (2012) 409–421.
[14] X.F. Li, X.L. Huai, J. Cai, F.Q. Zhong, X.J. Fan, Z.X. Guo, Convective heat transfer characteristics of China RP-3 aviation kerosene at supercritical pressure, Appl. Therm. Eng. 31 (2011) 2360–2366.
[15] Z. Tao, Y.C. Fu, G.Q. Xu, H.W. Deng, Z.X. Jia, Thermal and element analyses for supercritical RP-3 surface coke deposition under stable and vibration conditions, Energy Fuels 29 (2015) 2006–2013.
[16] G.Z. Liu, X.Q. Wang, X.W. Zhang, Pyrolytic depositions of hydrocarbon aviation fuels in regenerative cooling channels, J. Anal. Appl. Pyrolysis 104 (2013) 384–395.
[17] Y. Jiao, A.K. Liu, C.Y. Li, J.L. Wang, Q. Zhu, X.Y. Li, Y.Q. Chen, Catalytic cracking of RP-3 jet fuel over wall-coated Pt/ZrO_2–TiO_2–Al_2O_3 catalysts with different Al_2O_3 ratios, J. Anal. Appl. Pyrolysis 11 (2015) 100–107.
[18] G.Z. Zhao, W.Y. Song, R.L. Zhang, Effect of pressure on thermal cracking of china RP-3 aviation kerosene under supercritical conditions, Int. J. Heat Mass Transf. 84 (2015) 625–632.
[19] Y.C. Ju, G.Q. Xu, J. Guo, Y.J. Wang, Effects of pressure on the coking characteristic of jet fuel RP-3, J. Beijing Univ. Aeronaut. Astronaut. 3 (2010) 257–260.
[20] Y.J. Wang, G.Q. Xu, H.W. Wu, H.W. Deng, X. Luo, Experimental investigation of RP-3 thermal oxidation stability, J. Eng. Thermophys. 10 (2009) 1710–1712.
[21] L.G. Yuan, H.W. Deng, G.Q. Xu, Z.X. Jia, Y.F. Li, Effects of RP-3 coke deposition on heat transfer under supercritical pressure, J. Aerosp. Power 28 (2013) 832–837.
[22] Z.X. Jia, G.Q. Xu, J. Wen, Experimental study of the influence of surface coke deposition on heat transfer of aviation kerosene RP-3 at supercritical pressure, in: ASME 2012 International Mechanical Engineering Congress and Exposition, American Society of Mechanical Engineers, 2012, pp. 1927–1933.
[23] G.Z. Liu, Y.J. Han, L. Wang, X.W. Zhang, Z.T. Mi, Solid deposits from thermal stressing of n-dodecane and Chinese RP-3 jet fuel in the presence of several initiators, Energy Fuels 23 (2009) 356–365.
[24] G.Z. Liu, Y. Zhu, X. Zhang, et al., Role of dibenzyl diselenides in supercritical thermal cracking of jet fuel RP-3 as a coke inhibitor, J. Tianjin Univ. 11 (2007) 014.
[25] W. Guo, X.W. Zhang, G.Z. Liu, J. Wang, J. Zhao, Z.T. Mi, Roles of hydrogen donors and organic selenides in inhibiting solid deposits from thermal stressing of n-dodecane and Chinese RP-3 jet fuel, Ind. Eng. Chem. Res. 48 (2009) 8320–8327.
[26] M.A. Mawid, T.W. Park, B. Sekar, C.A. Arana, Development of detailed chemical kinetic mechanisms for ignition/oxidation of JP-8/Jet-A/JP-7 fuels, in: Proceedings of ASME Turbo Expo, 2003. Atlanta, Georgia, USA.
[27] D.B. Lenhert, D.L. Miller, N.P. Cernansky, The oxidation of JP-8, Jet-A, and their surrogates in the low and intermediate temperature regime at elevated pressures, Combust. Sci. Technol. 179 (2007) 845–861.
[28] T.R. Bott, Fouling of Heat Exchangers, Elsevier Science & Technology Books, 1995.
[29] H. Strawson, A. Lewis, Predicting Fuel Requirements for the Concorde, SAE 68-0734 (1968), http://dx.doi.org/10.4271/680734.
[30] Z.H. Liu, Q.C. Bi, Y. Guo, X.S. Ma, Z.Q. Yang, J.G. Yan, S.L. Hu, Hydraulic and thermal effects of coke deposition during pyrolysis of hydrocarbon fuel in a mini-channel, Energy Fuels 26 (2012) 3672–3679.
[31] J.L. Van Noord, B.R. Stiegemeier, Thermal Stability and Heat Transfer Investigation for Hydrocarbon Boost Engines, NASA Report, 2010. NASA/TM, 2010-216917.

[32] N. Gascoin, G. Abraham, P. Gillard, Thermal and hydraulic effects of coke deposit in hydrocarbon pyrolysis process, J. Thermophys. Heat Transf. 26 (2012) 57–65.
[33] Z.H. Liu, Q.C. Bi, J.T. Feng, Evaluation of heat sink capability and deposition propensity of supercritical endothermic fuels in a minichannel, Fuel 158 (2015) 388–398.
[34] Z.H. Liu, Q.C. Bi, Onset and departure of flow boiling heat transfer characteristics of cyclohexane in a horizontal minichannel, Int. J. Heat Mass Transf. 88 (2015) 398–405.
[35] Z.H. Liu, Q.C. Bi, Z.Q. Yang, Y. Guo, J.G. Yan, Critical heat flux of cyclohexane in uniformly heated minichannels with high inlet subcooling, Exp. Therm. Fluid Sci. 63 (2015) 106–114.
[36] Z.H. Liu, Q.C. Bi, Y. Guo, J.G. Yan, Z.Q. Yang, Convective heat transfer and pressure drop characteristics of near-critical-pressure hydrocarbon fuel in a mini-channel, Appl. Therm. Eng. 51 (2013) 1047–1054.
[37] Z.H. Liu, Q.C. Bi, Y. Guo, Q.H. Su, Heat transfer characteristics during subcooled flow boiling of a kerosene kind hydrocarbon fuel in a 1 mm diameter channel, Int. J. Heat Mass Transf. 55 (2012) 4987–4995.
[38] Z.H. Liu, Q.C. Bi, X.S. Ma, Y. Guo, S.J. Zhao, Thermal induced static instability of hydrocarbon fuel in the regeneratively cooled structures of hypersonic vehicles, in: 18th AIAA/3AF International Space and Hypersonic Systems and Technologies Conference, 2012. AIAA 2012-5759.